Bulletin of Volcanology (2024) 86:2
https://doi.org/10.1007/s00445-023-01690-9

SHORT SCIENTIFIC COMMUNICATION

Repeated Early Holocene eruptions of Katla, Iceland, limit the temporal resolution of the Vedde Ash

David J. Harning[1] · Thor Thordarson[2] · Áslaug Geirsdóttir[2] · Gifford H. Miller[1,3] · Christopher R. Florian[4]

Received: 28 August 2023 / Accepted: 19 November 2023 / Published online: 4 December 2023

Abstract

The Vedde Ash, originating from the Katla central volcano, Iceland, and taken to be dispersed across the North Atlantic and Europe at ~ 12 ka BP, is widely used as a geochronological marker. However, distal tephra layers with compositions like the Vedde Ash but of younger ages question the reliability of Vedde-like tephra layers as robust age control. Vedde-like tephra layers are rare in Icelandic sedimentary sequences and, where present, lack firm age control. Providing well-constrained local records of Early Holocene Katla layers is therefore critical to assess uncertainties related to the use of the Vedde Ash. Here we report three visible and stratigraphically separated Early Holocene Katla tephra layers from Torfdalsvatn, a lake in north Iceland, each with chemistry similar to the Vedde Ash. Using high-resolution ^{14}C chronologies, we provide ages ($\pm 1\sigma$) for these tephra layers of 11,315 ± 180, 11,295 ± 195, and 11,170 ± 195 cal a BP. These observations reinforce that multiple explosive eruptions of Katla occurred over a 1000-year interval in the Early Holocene and challenge the precision of some paleoclimate records using the Vedde Ash as a geochronometer where age control is equivocal. This may lead to a re-evaluation of age models for some Early Holocene North Atlantic records.

Keywords Iceland · Holocene · Tephra · Katla

Introduction

The Vedde Ash was first described in lake sediments from the Ålesund and Nordfjord regions of western Norway (Mangerud et al. 1984). Since then, it has been used as a widespread marker, present as a visible layer or cryptotephra in Greenland ice cores (e.g., Cook et al. 2022) and North Atlantic and Europe sedimentary records (Lane et al. 2011; Bronk Ramsey et al. 2015; Haflidason et al. 2018). In distal locations, its composition is generally rhyolitic. However, some sites, including the type locality in Norway, also contain a substantial and rather diverse mafic component (Mangerud et al. 1984; Birks et al. 1996; Davies et al. 2001; Koren et al. 2008; Lane et al. 2012). Bayesian modeling of radiocarbon ages from sediments in Europe places the time of Vedde Ash deposition at 12,023 ± 43 cal a BP (Bronk Ramsey et al. 2015), which is statistically indistinguishable to the age determined from layer counting in Greenland ice cores (12,121 ± 114 cal a BP, Rasmussen et al. 2006). Given that the Vedde Ash lies within the middle of the Younger Dryas Stadial (or Greenland Stadial 1, 12,900 to 11,700 cal a BP, Rasmussen et al. 2006), an abrupt cold event within the Late Glacial to Holocene transition (Mangerud et al. 1974), studies have leveraged its age and widespread distribution to synchronize North Atlantic paleoclimate records and assess leads/lags in the past climate system (Bakke et al. 2009; Lane et al. 2013).

While the Vedde Ash 's composition and analytical age constraint have been relied on for age control, other compositionally similar tephra layers from the Katla volcano have also been identified in the Late Glacial to Early Holocene period (e.g., Lane et al. 2012). These include but are not limited to the Dimna Ash (> 15,100 cal a BP, Koren et al.

Editorial responsibility: J. L. Smellie

✉ David J. Harning
david.harning@colorado.edu

[1] Institute of Arctic and Alpine Research, University of Colorado Boulder, Boulder, CO, USA

[2] Faculty of Earth Sciences, University of Iceland, Reykjavík, Iceland

[3] Department of Geological Sciences, University of Colorado Boulder, Boulder, CO, USA

[4] National Ecological Observatory Network, Boulder, CO, USA

2008), the Abernethy Tephra (11,790 to 11,200 cal a BP, Macleod et al. 2015), the Suduroy Tephra (8160 to 7880 cal a BP, Wastegård 2002), as well as tephra glass found on the South Iceland Rise that may be up to 3000 years older than the Vedde Ash (Bond et al. 2001; Thornalley et al. 2011). However, few sites in Iceland contain these silicic Katla tephra layers, presumably due to substantial ice sheet presence through the Younger Dryas that lingered into the Early Holocene (e.g., Patton et al. 2017). Based on compositional similarities, correlations have been proposed between the Skógar Tephra in north Iceland (Norðdahl and Haflidason 1992) and the Sólheimar Ignimbrite adjacent to Katla volcano have been proposed (Lacasse et al. 1995), but these deposits lack independent age control needed for confirmation. The Sólheimar Ignimbrite is present as outcrops on the southern flanks of Katla, implying that these slopes were ice-free when it was formed, ruling out a Younger Dryas or older age due to local ice sheet cover at this time (Geirsdóttir et al. 2000, 2022). Furthermore, the Sólheimar Ignimbrite also lacks the basaltic component present in the Vedde Ash at its type locality and features a distinct intermediate component (Lane et al. 2012; Tomlinson et al. 2012).

Torfdalsvatn, a lake in north Iceland (66.06° N, 20.38° W, Fig. 1a), contains the longest known lake sedimentary record in Iceland. Based on conventional radiocarbon (^{14}C) ages and tephra layer compositional analysis, Torfdalsvatn's record has been suggested to include the Vedde Ash, among others (Björck et al. 1992; Rundgren 1995). However, these records precede recent advancements in ^{14}C calibration as well as the recognition of multiple silicic Katla tephra layers during the Late Glacial period. Here we present new and expanded compositional datasets of tephra layers from Torfdalsvatn's earliest sediment, and improved age control based on new ^{14}C ages, updated radiocarbon calibration curves (Reimer et al. 2020), and Bayesian modeling (Bronk Ramsey 2009; Blaauw and Christen 2011). We argue that contrary to conclusions in earlier studies, Torfdalsvatn does not contain the Vedde Ash. Instead, our results show that three visible tephra layers in Torfdalsvatn's oldest sediment have similar geochemical composition to the Vedde Ash but are significantly younger, which may limit the utility of similar tephra found in distal settings as precise chronometers (e.g., Lane et al. 2012).

Materials and methods

Sediment core collection

In February 2012, we recovered a continuous lake sediment core (TORF12-1A-1B) using a Bolivia coring system from a lake-ice platform above the deepest part of the lake (5.8 m depth, Fig. 1b). TORF12-1A-1B was collected in 1.5 m increments until reaching deglacial sediment and bedrock refusal at the bottom. For this study, we focus on the deepest segment, which contains visible tephra layers deposited shortly after local deglaciation (Fig. 2). Another

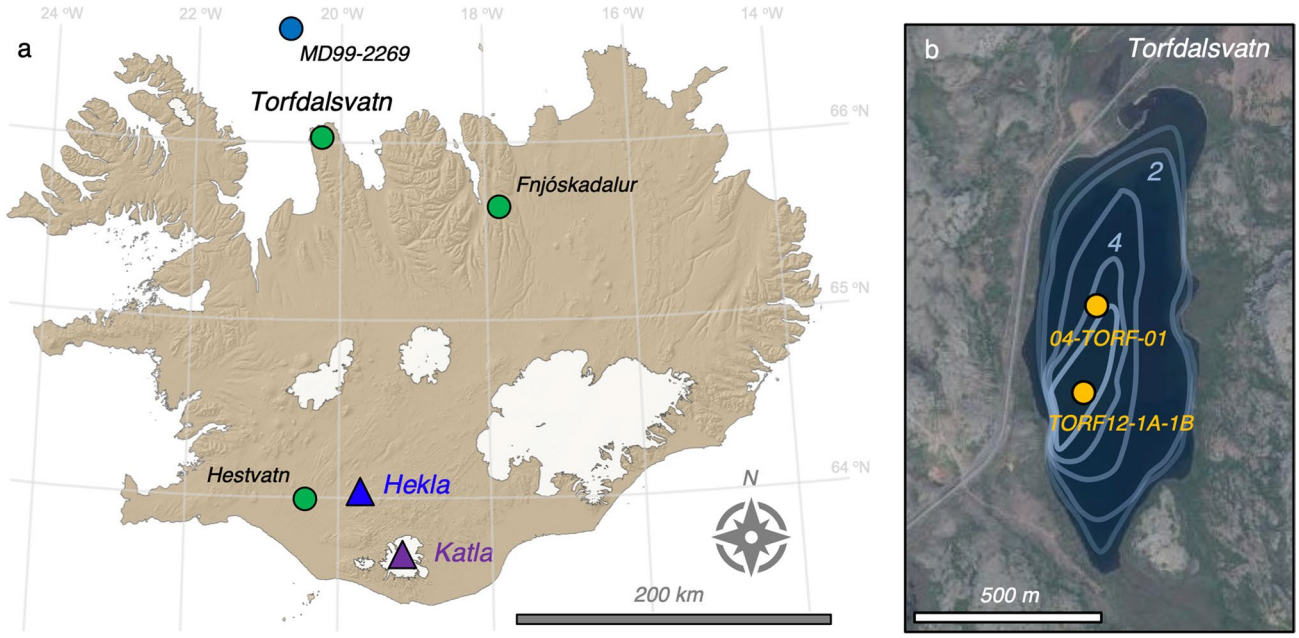

Fig. 1 Overview map of Iceland. **a** Locations of Katla and Hekla central volcanos (triangles) and terrestrial (green) and marine sites (blue) mentioned in the text. **b** Close-up of Torfdalsvatn, its bathymetry (1-m isolines, Axford et al. 2007), and location of lake sediment core sites for TORF12-1A-1B (this study) and 04-TORF-01 (Axford et al. 2007). Base imagery courtesy of Loftmyndir ehf

sediment core from a shallower part of the lake was collected using a Nesje coring system in 2004 (04-TORF-01, Fig. 1b), which reaches deglacial sediment at the base (Axford et al. 2007). Images of 04-TORF-01 were taken at the University of Minnesota's LacCore facility and capture the relative stratigraphy of core TORF12-1A-1B in high resolution (Fig. 2).

Tephra compositional analysis

From TORF12-1A-1B, 4 visible tephra layers were sampled at 845, 837, 835.5, and 827 cm depth, sieved to isolate glass fragments between 125 and 500 µm, and embedded in epoxy plugs. Individual glass shards (n = 142) were analyzed at the University of Iceland on a JEOL JXA-8230 election microprobe using an acceleration voltage of 15 kV, beam current of 10 nA, and beam diameter of 10 µm. The international A99 (mafic) and Lipari obsidian (felsic) standards were used to monitor for instrumental drift and maintain consistency between measurements (Table S1, Supplemental Data). Tephra origin was assessed using the systematic procedures outlined in Jennings et al. (2014) and Harning et al. (2018) that is underpinned by an extensive compilation of glass compositions (> 10,000 mostly published analyses)

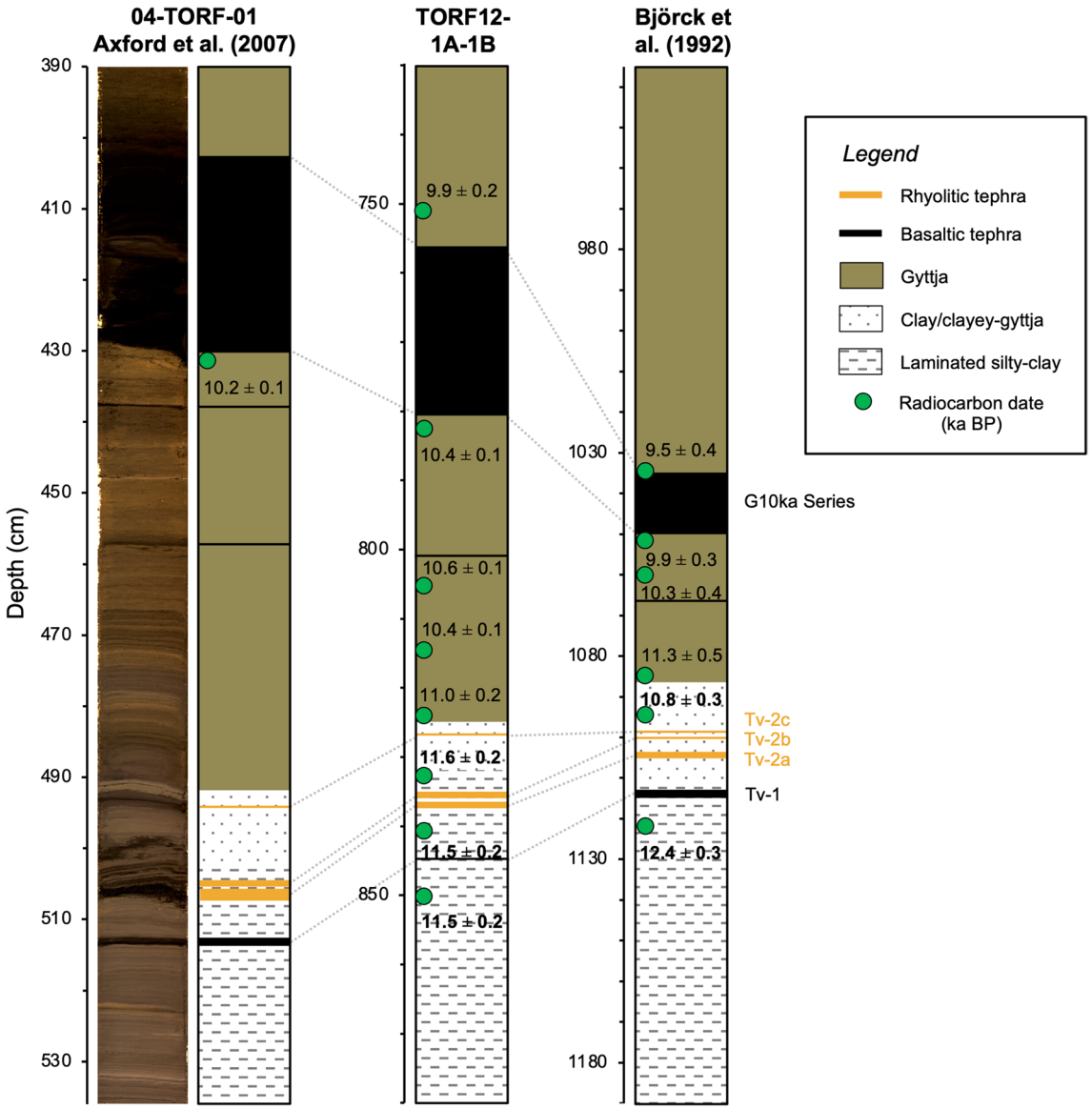

Fig. 2 Simplified stratigraphy of lake sediment core TORF12-1A-1B (middle) compared to 04-TORF-01 (Axford et al. 2007) and that from Björck et al. (1992). Correlation of this study's key tephra layers is indicated with dotted gray lines. Sediment core images for 04-TORF-01 taken at the University of Minnesota's LacCore facility, and close-up images of the tephra layers are provided in the Supplemental Material (Fig. S2). See Table 1 for complete radiocarbon information from all three sediment cores

of tephra from key proximal locations in Iceland, representing all tephra-producing volcanic systems. Briefly, based on SiO_2 wt% vs total alkali ($Na_2O + K_2O$) wt%, we determine whether the tephra volcanic source is mafic (tholeiitic or alkalic), intermediate, and/or rhyolitic. We then objectively discriminate the source volcanic system through a detailed series of bi-elemental plots produced from available compositional data on Icelandic tephra (Fig. S1, Supplemental Data).

In addition to the 4 tephra layers analyzed by electron microprobe above, we also use the G10ka Series (formerly Saksunarvatn Ash), which has been geochemically identified in previous Torfdalsvatn records (Björck et al. 1992; Alsos et al. 2021), and is easily identifiable by its > 20 cm thickness and coarse-grained nature (Fig. 2, 755 to 781 cm depth). However, instead of using the single age from the Greenland ice core (e.g., Alsos et al. 2021), we apply an age of 10,400 cal a BP to the lower limit based on the recent recognition that it was generated from multiple eruptions between 10,400 and 9900 cal a BP (e.g., Jennings et al. 2014; Harning et al. 2018, 2019; Óladóttir et al. 2020).

Radiocarbon

We obtained 10 bulk sediment ^{14}C dates from Torfdalsvatn, 8 from TORF12-1A-1B (Table 1) and 2 from a neighboring core (TORF12-2A, Table S4, Supplemental Material). As bulk sediment ^{14}C in Icelandic lakes may be stratigraphically too old due to the introduction of old carbon from the catchment (Geirsdóttir et al. 2009), the latter two dates, which straddle the well-dated Hekla 4 tephra (4,260 cal a BP, Dugmore et al. 1995; Florian 2016), are used to test the reliability of bulk sediment ^{14}C dates in Torfdalsvatn. All bulk sediment ^{14}C dates were processed in the Arizona Climate and Ecosystem (ACE) Isotope Laboratory, Northern Arizona University. Samples were acidified with HCl to remove carbonate, combusted at 1030 °C into CO_2 with an elemental analyzer (vario ISOTOPE select, Elementar), and then analyzed on a Mini Carbon Dating System (MICADAS, IonPlus). All results were corrected for isotopic fractionation according to conventions of Stuiver and Polach (1977), with $\delta^{13}C$ values measured on prepared graphite using the AMS spectrometer. These latter values can differ from sample $\delta^{13}C$ values and are therefore not reported.

Age modeling

Before constructing age models for the Björck et al. (1992) and TORF12-1A-1B sediment records, we tested for the possibility of temporal outliers using Outlier Analysis, an objective Bayesian statistical analysis (Bronk Ramsey 2009), in OxCal v4.4 (Bronk Ramsey 2023). Age models for the Björck et al. (1992) and TORF12-1A-1B sediment records were then created using the R package rbacon, default settings (Fig. 3; Blaauw and Christen 2011; R Core Team 2021), and the IntCal20 calibration curve (Reimer et al. 2020).

Results and interpretations

Lithostratigraphy

For TORF12-1A-1B, we divide the lithostratigraphy into five units: laminated silty-clay, clay/clayey-gyttja, gyttja, visible basaltic tephra, and visible rhyolitic tephra (Fig. 2).

Table 1 New and previously published lake sediment radiocarbon information used in this study

Lab ID	Depth (cm)	Material	Conventional ^{14}C age ± σ	Calibrated age BP ± σ	Reference
NAU ACE 3914.1.1	750	Bulk sediment	8815 ± 95	9910 ± 215	This study
NAU ACE 3915.1.1	783	Bulk sediment	9175 ± 93	10,365 ± 120	This study
NAU ACE 3916.1.1	804	Bulk sediment	9357 ± 91	10,565 ± 140	This study
NAU ACE 3917.1.1	814	Bulk sediment	9274 ± 93	10,435 ± 135	This study
NAU ACE 3918.1.1	824	Bulk sediment	9721 ± 94	11,035 ± 210	This study
NAU ACE 3919.1.1	833	Bulk sediment	10,053 ± 104	11,580 ± 225	This study
NAU ACE 3920.1.1	843	Bulk sediment	9982 ± 93	11,475 ± 205	This study
NAU ACE 3921.1.1	850	Bulk sediment	10,041 ± 95	11,545 ± 195	This study
Ua-1892	1035	Bulk sediment	8540 ± 230	9520 ± 370	Björck et al. (1992)
Ua-1891	1052	Bulk sediment	8860 ± 250	9880 ± 320	Björck et al. (1992)
Ua-1890	1060	Moss macrofossil	9180 ± 210	10,330 ± 370	Björck et al. (1992)
Ua-1889	1085	Bulk sediment	9890 ± 290	11,340 ± 540	Björck et al. (1992)
Ua-1888	1095	Bulk sediment	9470 ± 200	10,800 ± 290	Björck et al. (1992)
Ua-1887	1122	Bulk sediment	10,550 ± 240	12,400 ± 340	Björck et al. (1992)
NSRL-14518	432	Humic acid	9100 ± 25	10,240 ± 10	Axford et al. (2007)

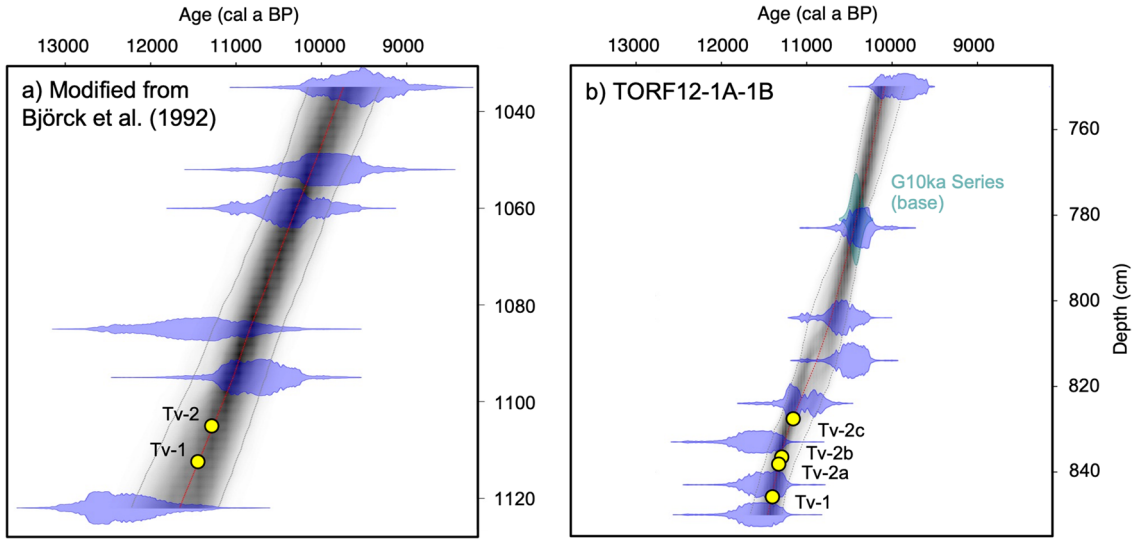

Fig. 3 Torfdalsvatn lake sediment age models for **a** Björck et al. (1992) based on six ^{14}C ages (blue), and **b** TORF12-1A-1B based on eight ^{14}C ages (blue) and one marker tephra layer (green). Tephra layers ages constrained from these models are marked in yellow. Red lines reflect mean values of model iterations, the gray lines denote the 95% confidence envelope, and darker shading reflects more likely ages. See Table 1 for complete radiocarbon information

The base of the core at 879 cm up to 834 cm depth is comprised of laminated silty-clay. Above the basal unit, from 834 to 824 cm, is clay/clayey-gyttja. The deepest part of sediment core 04-TORF-01, which correlates to TORF12-1A-1B (Fig. 2), is further characterized by high magnetic susceptibility and low organic carbon (< 1%) (Axford et al. 2007), which along with the intermittent laminations are consistent with Icelandic lake sediments deposited in a freshly deglaciated environment (e.g., Larsen et al. 2012; Harning et al. 2016; Geirsdóttir et al. 2022). The remainder of both sediment cores is comprised of organic gyttja, and from core 04-TORF-01, relatively low magnetic susceptibility and high organic carbon up to 8%, all consistent with a non-glacial catchment and productive aquatic system (Axford et al. 2007). Throughout all units, there are intercalated tephra layers of varying thickness and color. The tephra layers sampled and analyzed in this study are located at 845, 837, 835.5, and 827 cm depth. The relative stratigraphy of core TORF12-1A-1B is well replicated in core 04-TORF-01 and the core from Björck et al. (1992), with the primary differences being the overall length of each sediment record (Fig. 2). 04-TORF-01 was collected from a slightly shallower region of the lake where less sediment accumulation is expected compared to the depocenter of the lake where TORF12-1A-1B was collected from (Fig. 1b). Björck et al. (1992) do not report their coring location. However, based on our team's collective experience coring Torfdalsvatn since 2004, where no records have exceeded 900 cm length, the overall length of the Björck et al. (1992) sediment core (1195 cm) is longer than expected, possibly due to angling of the coring device during collection.

Chronology

Calibrated age models for the sediment record of Björck et al. (1992) and TORF12-1A-1B both show linear sedimentation rates (Fig. 3), and outlier analysis confirms that neither sediment core has ^{14}C outliers (Table S3 and S4, Figs. S3 and S4). While both records show similar and slight age reversals of mean ^{14}C ages (NAU ACE 3916.1.1 and 3917.1.1, this study; Ua-1889 and 1888, Björck et al. 1992, Table 1), their uncertainties substantially overlap and are not identified as problematic through their posterior probabilities determined through Outlier Analysis (Tables S3 and S4) or bacon age models (Fig. 3).

Bulk sediment ^{14}C ages above (4305 ± 115 cal a BP) and below (4675 ± 90 cal a BP) the Hekla 4 tephra layer (4260 cal a BP, Dugmore et al. 1995) in Torfdalsvatn (Table S5) show minimal differences between ^{14}C ages and the acknowledged age of Hekla 4 on the order of centuries. Similarly, bulk sediment ^{14}C ages above (9910 ± 215 cal a BP) and below (10365 ± 120 cal a BP) the G10ka Series tephra (Fig. 2) are consistent with independent age estimates for these tephra units that range from 10,400 to 9900 cal a BP (Óladóttir et al. 2020). Possible uncertainties in bulk sediment ^{14}C ages in Iceland can result from the introduction of inorganic carbon (geothermal activity) and old organic carbon (erosion) (e.g., Geirsdóttir et al. 2009; Ascough et al. 2011). While lakes located in the

active volcanic zone show a freshwater reservoir effect, where ^{14}C ages are influenced by CO_2 delivered by geothermally mediated groundwater (Ascough et al. 2011), Torfdalsvatn's location is well outside active volcanic zones in Iceland and thus removed from major geothermal activity (Flóvenz and Sæmundsson 1993). Consequently, the influence of such activity on the lake water ^{14}C is minimal. In a freshly deglaciated landscape, like we infer from Torfdalsvatn's sediment characteristics, old organic carbon was likely removed entirely by the pre-existing ice sheet, making erosion of stratigraphically old organic carbon into the lake improbable as well. The minimal differences between the age of the Hekla 4 and G10ka Series tephra layers and bounding bulk sediment ^{14}C ages reinforce this conclusion and suggest that the bulk sediment ^{14}C ages from Torfdalsvatn's basal section provide reliable *maximum* ages of sedimentary deposition and age constraint for the intercalated Early Holocene tephra layers.

Tephra layer descriptions

12TORF-1B-108 (Tv-1)

A 0.6 cm thick, black basalt tephra of very fine ash is present at 845 cm depth (Table 1, Fig. 2) and has a modeled age of 11,390 ± 180 cal a BP (Fig. 3b). The tephra layer is comprised of pristine and vesicular, sideromelane grains, poorly to non-vesicular black translucent to opaque grains, and grey microcrystalline grains. All 17 grains analyzed have alkalic basalt composition consistent with the Hekla volcanic system (Fig. 4a and S1; Table S2). The similar homogenous composition and thickness to the lowermost tephra layer described by Björck et al. (1992) correlate this to the Tv-1 tephra layer (Fig. 4a).

12TORF-1B-100 (Tv-2a)

A 1.1 cm thick, black and white (i.e., salt and pepper textured) layer of medium grain ash is located at 837 cm depth (Fig. 2) and has a modeled age of 11,315 ± 180 cal a BP (Fig. 3b). The tephra layer has sharp upper and lower contacts with surrounding sediment (Fig. 2) and is comprised of silicic and basaltic grains with delicate protrusions (Fig. 5a). The 41 grains analyzed are alkalic in composition and consistent with the Katla volcanic system (Fig. 4b, c and S1; Table S2). These range from basalt ($n = 20$) to low-SiO_2 ($n = 2$) and high-SiO_2 intermediate ($n = 1$), to rhyolite ($n = 18$). The similar bimodal compositional range (Fig. 4b) and thickness between the 12TORF-1B-100 tephra and the Tv-2 tephra described by Björck et al. (1992) support a correlation.

12TORF-1B-99 (Tv-2b)

A 0.9 cm thick, black and white layer (i.e., salt and pepper textured) of medium grain ash is located at 835.5 cm depth (Fig. 2) and has a modeled age of 11,295 ± 195 cal a BP (Fig. 3b). The tephra layer has sharp upper and lower contacts with surrounding sediment (Fig. 2) and is comprised of silicic and basaltic grains featuring delicate protrusions (Fig. 5b). All 44 grains analyzed exhibit alkalic compositions consistent with the Katla volcanic system (Fig. 4 and S1; Table S2). These range from basalt ($n = 19$) to low-SiO_2 ($n = 4$) and high-SiO_2 intermediates ($n = 2$), and rhyolites ($n = 19$). This bimodal compositional range is identical to that of the Tv-2a tephra below (Fig. 4b). Although not analyzed for composition in Björck et al. (1992), the authors note the presence of two tephra horizons above Tv-2, which we correlate to Tv-2b and Tv-2c in TORF12-1A-1B based on stratigraphic position (Fig. 2).

12TORF-1B-90 (Tv-2c)

A 0.4 cm thick, dark layer of fine to medium grain ash is located at 827 cm depth (Fig. 2) and has modeled age of 11,170 ± 195 cal a BP (Fig. 3b). While the tephra layer has sharp upper and lower contacts with surrounding sediment (Fig. 2), there is a minor component of lithic and crystal fragments (Fig. 5c), which likely results from sampling-induced contamination due to the thin nature of the tephra layer. Of the 40 grains analyzed, 33 (83%) exhibit alkalic compositions, where the composition of 28 grains indicates origin from Katla, while five alkali basalt grains are consistent with the Hekla volcanic system (Fig. 4). The dominant Katla tephra grains range from basalt ($n = 7$) to basaltic icelandite to icelandite ($n = 3$) and rhyolite ($n = 18$). The seven tholeiite basalt tephra grains are consistent with origin from the Kverkfjöll volcanic system (Fig. S1 and Table S2). The presence of non-Katla tephra grains likely reflects similarly timed eruptions from the Kverkfjöll and Hekla volcanic systems.

Discussion

Evidence for primary tephra deposits

Torfdalsvatn's stratigraphic record includes four distinct Early Holocene tephra layers (Fig. 2). The lowermost layer has a Hekla basalt composition (Tv-1, Fig. 4a), and the uppermost three have bimodal Katla chemical composition (Tv-2a, Tv-2b, and Tv-2c, Fig. 4b–d). Previous lake sediment studies from Torfdalsvatn suggest that the 9 cm of sediment immediately following the first silicic Katla tephra layer (Tv-1), which includes two unanalyzed tephra layers

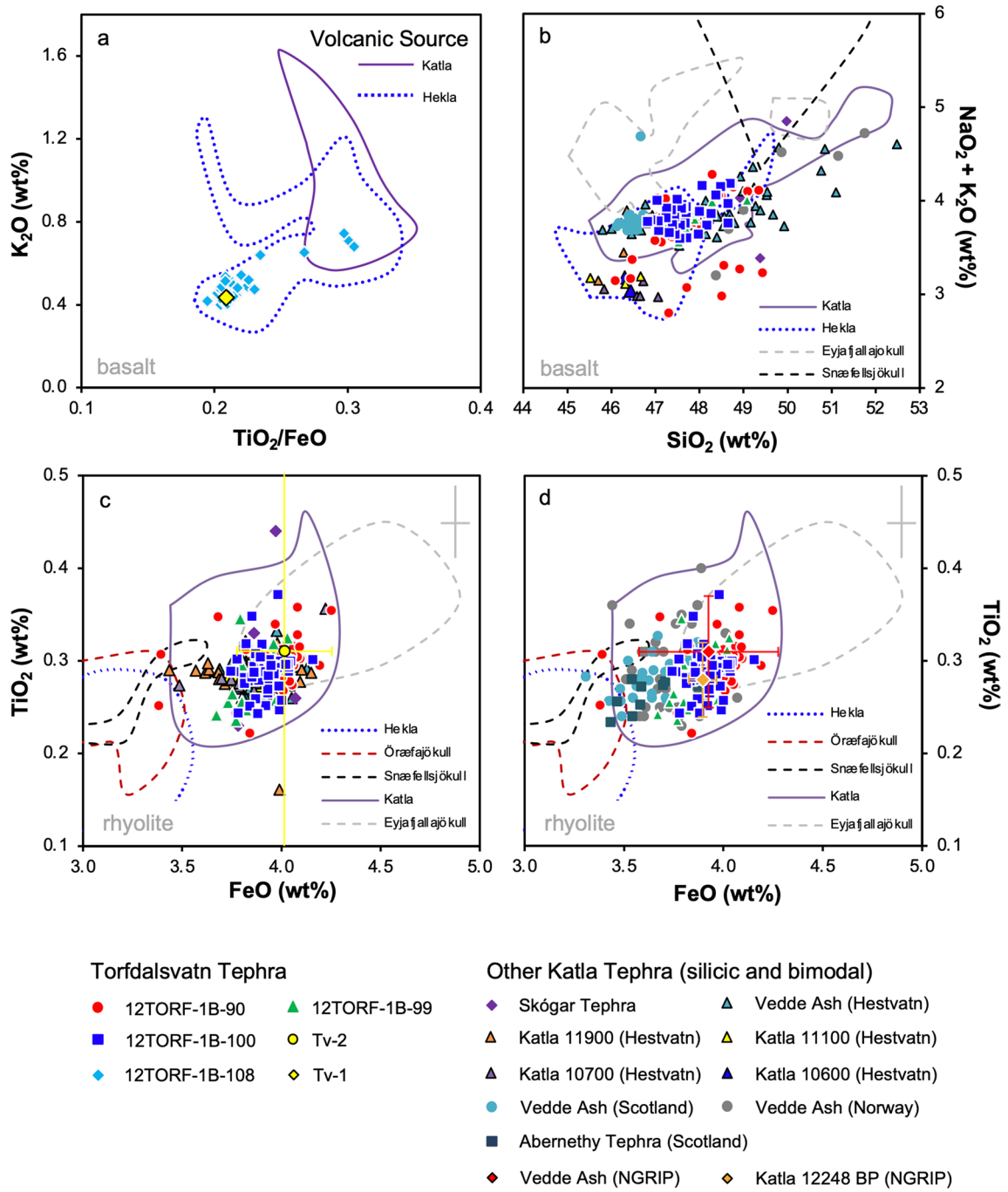

Fig. 4 Example source discrimination biplots. **a** Basaltic Hekla Tv-1 tephra, **b** basaltic Katla tephra layers endmembers in Torfdalsvatn compared with similar tephra layers from Iceland and Europe (Norðdahl and Haflidason 1992; Lane et al. 2012; Geirsdóttir et al. 2022), **c** rhyolitic Katla tephra layer endmembers in Torfdalsvatn compared with similar tephra layers from Iceland (Björck et al. 1992; Norðdahl and Haflidason 1992; Geirsdóttir et al. 2022), and **d** Greenland and Europe (Mortensen et al. 2005; Matthews et al. 2011; Lane et al. 2012). Tv-1, Tv-2, and NGRIP tephra layer geochemistries are average values and standard deviations (Björck et al. 1992; Mortensen et al. 2005). Uncertainty from standard analyses shown in upper right corners of **c** and **d** (light gray). Please see the supporting data for raw data and further discrimination plots

correlated to Tv-2b and Tv-2c (Fig. 2), resulted from redeposition of older sediments based on similar pollen spectra to those in lower levels (Björck et al. 1992; Rundgren 1995). However, this does not require the sediment to be reworked and could simply be due to the presence of similar plant assemblages in the catchment. Moreover, based

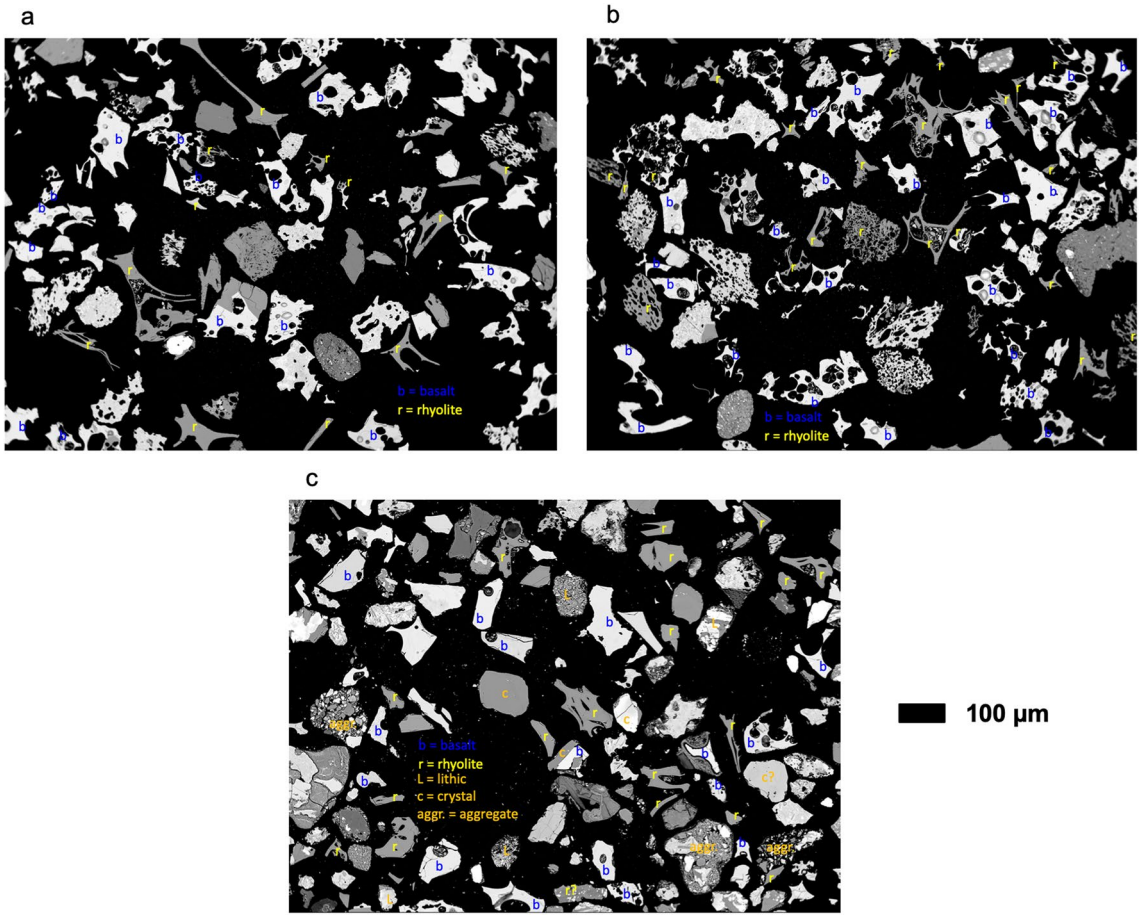

Fig. 5 Electron microprobe backscatter images for **a** Tv-2a (TORF-1B-100), **b** Tv-2b (TORF-1B-99), and **c** Tv-2c (TORF-1B-90)

on the sediment lithostratigraphy ("Lithostratigraphy" section), the landscape was freshly deglaciated, suggesting there was minimal development of catchment soil and vegetation available for redeposition. In distal regions, shard counting is often used to identify cryptotephra layers not visible to the naked eye (maximum shard count) and evaluate the possibility of reworked tephra sequences (e.g., Lowe 2011). However, in proximal volcanic regions, such as Iceland, the presence of pure, visible tephra layers will result in orders of magnitude higher counts in the tephra layers compared to background sediment, which itself is often comprised of tephra due to the volcanic origin of Icelandic soil (Arnalds 2004).

For proximal volcanic locations, tephra grain morphology and rounding are key tools to differentiate between primary and reworked tephra layer deposits (Wilcox and Naeser 1992; Leahy 1997; Gudmundsdóttir et al. 2011; Lowe 2011; Óladóttir et al. 2011). Primary tephra layers also feature (1) sharp contacts, (2) uniform geochemical compositions, (3) minimal incorporation of exotic material (e.g., lithic fragments, biological microfossils), (4) lack of sedimentary structure such as turbidites and discontinuous layers, and (5) spatial distribution of the layer across different locations (Lacasse et al. 1998; Boygle 1999; Shane et al. 2006; Gudmundsdóttir et al. 2011; Lowe 2011). Based on these criteria, we argue that all three tephra layers are primary deposits. Specifically, the three Katla tephra layers in Torfdalsvatn have sharp contacts separated by non-volcanic sediment (Fig. S2), tight geochemical populations (Fig. 4), non-rounded shard morphometry (Fig. 5), do not contain substantial exotic material, feature large grain sizes (Fig. 5) that cannot be readily mobilized by wind, feature depositional textures and structures that are not compatible with deposition via turbidity currents, are present in all three sediment records from the same lake (Fig. 2) and possible correlations elsewhere around Iceland (see the "Possible correlations for Torfdalsvatn tephra layers in Iceland" section). The close similarity between bulk sediment ^{14}C ages bounding the well-dated G10ka Series and Hekla 4 tephra layers suggests that reworking of catchment material is minimal around Torfdalsvatn throughout the Holocene, particularly following tephra deposition, which is known to lead to intensified erosion in other Icelandic environments (e.g., Geirsdóttir et al. 2020). In conjunction with Bayesian

age modeling, these lines of evidence demonstrate that the three Early Holocene tephra layers found in Torfdalsvatn were generated from separate Katla eruptions between 11,315 ± 180 and 11,170 ± 195 cal a BP.

Torfdalsvatn Katla tephra layers are not correlated to the Vedde Ash

The oldest of the three Katla tephra layers in Torfdalsvatn (Tv-2a) was previously correlated to the Vedde Ash (Björck et al. 1992) and the local Skógar Tephra based on major oxide composition (Norðdahl and Haflidason 1992). However, the age of Tv-2a (11,315 ± 180 cal a BP) is inconsistent with the Vedde Ash found in Europe (12,023 ± 43 cal a BP, Bronk Ramsey et al. 2015) and Greenland (12,121 ± 114 cal a BP, Rasmussen et al. 2006) (Fig. 6). Moreover, while the silicic composition of the Vedde Ash in Greenland ice cores (Mortensen et al. 2005) resembles the layers in Torfdalsvatn, the Vedde Ash layers identified in Norway and Scotland (Lane et al. 2012) are compositionally different than those in Torfdalsvatn (Fig. 4d). For example, FeO wt% for a given TiO_2 wt% is lower for the Vedde Ash layers in Europe than for the three Torfdalsvatn tephra (Fig. 4d). While the bimodal Skógar Tephra, found ~ 120 km to the east of Torfdalsvatn in Fnjóskadalur (Fig. 1a) is compositionally similar to the Vedde Ash in Greenland and the three Katla tephra layers in Torfdalsvatn (Fig. 4b, c), there is no independent age control to support either correlation (Norðdahl and Haflidason 1992). Thus, our new compositional and chronological datasets demonstrate that none of the three tephra layers in Torfdalsvatn can be correlated with the Vedde Ash or Skógar Tephra at this time.

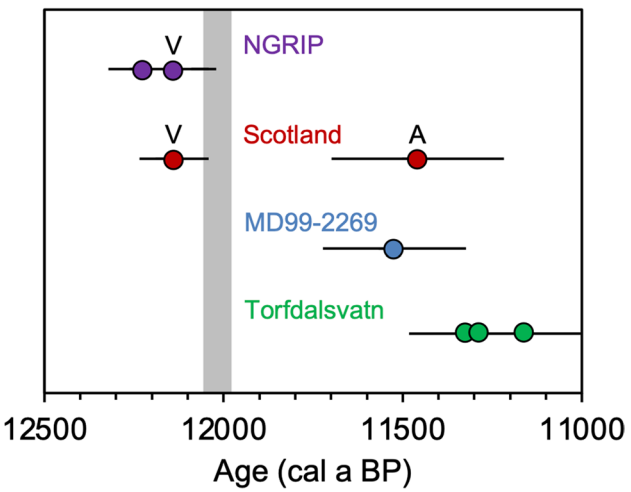

Fig. 6 Age and uncertainty of well-constrained Vedde Ash deposits and other compositionally similar Katla tephra from Greenland (purple, Rasmussen et al. 2006) and Scotland (red, Matthews et al. 2011) in comparison to the Early Holocene Katla tephra layers from MD99-2269 (blue, Kristjánsdóttir et al. 2007) and Torfdalsvatn (green, this study). V, Vedde Ash; A, Abernethy Tephra. Vertical gray bar corresponds to the Bayesian ^{14}C age modeling of European Vedde Ash layers (Bronk Ramsey et al. 2015)

Possible correlations for Torfdalsvatn tephra layers in Iceland

Tephra datasets from Iceland's marine and terrestrial realm provide possible correlations to the tephra layers identified in Torfdalsvatn. The ages of the three Katla tephra layers in Torfdalsvatn are similar to three rhyolitic Katla cryptotephras dated to 11,520 ± 190, 10,760 ± 100, and 10,420 ± 100 cal a BP in marine sediment core MD99-2269, immediately north of Torfdalsvatn on the North Icelandic Shelf (Figs. 1a and 6, Kristjánsdóttir et al. 2007). While the ages of the MD99-2269 tephra layers are hampered by unconstrained marine reservoir ages that prevent conclusive correlations with Torfdalsvatn, the presence of multiple, similar Katla tephra layers adds further support to the notion of three (or more) rhyolitic Katla tephra with northerly dispersal during the Early Holocene. In south Iceland, a lake sediment record from Hestvatn (Fig. 1a) contains four bimodal Katla tephra layers above the assumed Vedde Ash. All four have similar composition to the three tephra layers in Torfdalsvatn with ages between ~ 11,700 and 10,600 cal a BP (Fig. 4b, c, Geirsdóttir et al. 2022). In addition, there are two Hekla basalt tephra layers with similar age to Tv-1 (10,630 and 10,400 cal a BP, Geirsdóttir et al. 2022) that provide further correlation potential with Torfdalsvatn's tephra record. While there is relatively greater uncertainty in the age of Hestvatn's Katla tephra layers, as they were deposited in a shallow marine environment with high sediment accumulation rates (Geirsdóttir et al. 2022), it is possible that some may correlate with those in Torfdalsvatn. Future efforts to improve the chronological control of these marine and lake sediment records, as well as the identification of similar tephra layers in additional stratigraphic records in Iceland using major oxide as well as trace element composition, will be imperative to draw definitive correlations with the three tephra layers Torfdalsvatn and trace the ash plume trajectories from these Katla eruptions.

Repeated rhyolitic and bimodal tephra layers in the North Atlantic and Europe

Like Iceland, records from elsewhere in the North Atlantic and Europe indicate the presence of multiple Katla tephra layers with Vedde-like compositions during the Late Glacial and Early Holocene (Lane et al. 2012). In Greenland ice cores (e.g., NGRIP), another rhyolitic tephra layer from the Katla volcanic system (Fig. 4d) is estimated to be < 100 years older than the Vedde Ash (Mortensen et al. 2005; Cook et al. 2022; Fig. 6), similar to evidence in the marine realm

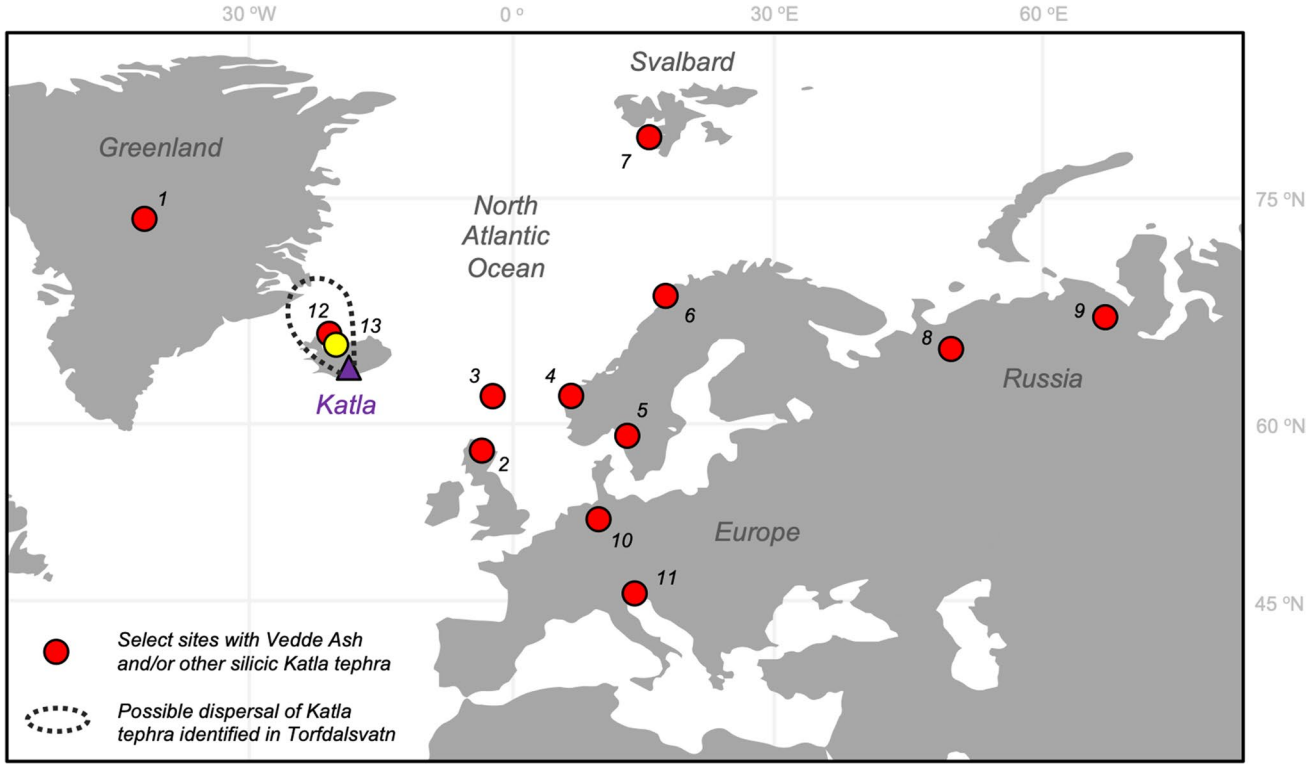

Fig. 7 Map of select sites with Vedde Ash and other similar rhyolitic Katla deposits. (1) NGRIP ice core (Mortensen et al. 2005), (2) Abernethy Forest, Scotland (Matthews et al. 2011; MacLeod et al. 2015), (3) MD99-2284 (Muschitiello et al. 2019), (4) Kråkenes, Norway (Mangerud et al. 1984), (5) Lake Madtjärn, Sweden (Wastegård et al. 1998), (6) Lofoten Islands, Norway (Pilcher et al. 2005), (7) Heftyevatnet (Farnsworth et al. 2022), (8) Lake Yamozero, Siberia (Haflidason et al. 2018), (9) Lake Bolshoye Shchuchye, Siberia (Haflidason et al. 2018), (10) Lake Hämelsee, Germany (Jones et al. 2018), (11) Lake Bled, Slovenia (Lane et al. 2011), (12) MD99-2269 (Kristjánsdóttir et al. 2007), and (13) Torfdalsvatn, Iceland (yellow). Dashed grey line denotes the possible northern dispersal of Katla tephra layers identified in Torfdalsvatn

between Iceland and Greenland (Eiríksson et al. 2004; Gudmundsdóttir et al. 2012; Voelker and Haflidason 2015). However, age constraints for the Vedde Ash in the latter cases near Iceland are either based solely on correlation of tephra compositional analysis (Eiríksson et al. 2004; Voelker and Haflidason 2015), or with ^{14}C ages that are too young for the Vedde Ash (Gudmundsdóttir et al. 2012), suggesting other potential tephra layer correlations, such as those from Torfdalsvatn, are *possible*. In south Sweden, two cryptotephra shard peaks associated with the Vedde Ash appear in lake sediment with ^{14}C ages of 12,045 to 11,975 cal a BP (Wastegård et al. 1998). In and around Scotland, the compositionally similar Abernethy Tephra (Fig. 4d) is ~ 600 years younger than the Vedde Ash (Fig. 6) as verified through high-resolution ^{14}C dates (Matthews et al. 2011; MacLeod et al. 2015; Muschitiello et al. 2019). In Lake Hämelsee, Germany, a cryptotephra, which possibly correlates to the Abernethy Tephra, as well as less concentrated glass shards of Vedde-like composition, is present above the assumed, but not independently dated, Vedde Ash (Jones et al. 2018). Tephra glass with Vedde composition found on the Lofoten Islands, Norway, is intermixed with the Askja S tephra layer, dated to 10,830 ± 57 cal a BP (Pilcher et al. 2005; Bronk Ramsey et al. 2015). Collectively, these records demonstrate that the record from Torfdalsvatn is not unique, and that the Katla volcanic system produced multiple tephra layers with similar rhyolitic and bimodal compositions in the millennia following the Vedde Ash.

These distal records also allow us to address *potential* dispersal patterns of Katla's multiple Early Holocene volcanic eruptions. In addition to slightly different compositions, the similarly aged Abernethy Tephra was not likely generated during the same eruption(s) that produced the tephra layers found in Torfdalsvatn. Rhyolitic tephra in Iceland is produced during explosive eruptions that feature eruption columns exceeding 20 km in altitude and transported distally by stratospheric winds (Thorarinsson 1950; Sharma et al. 2008; Carey et al. 2010). At least today, Icelandic ash plumes that reach the stratosphere are dispersed eastward by strong westerlies in the fall and winter. However, these stratospheric winds are seasonal, and in the spring and summer, the prevailing dispersal direction

shifts to relatively weak easterlies (Lacasse 2001). If stratospheric wind patterns were the same in the Early Holocene, the opposing trajectories of tephra dispersal to Torfdalsvatn and Europe (Fig. 7), as well as the short-lived nature of explosive rhyolitic eruptions (duration of individual events on the order of hours to days), makes it improbable that tephra layers found in both locations could have been generated from the same eruption. Future efforts mapping these tephra layers in additional North Atlantic records as well as detailed reconstructions of Holocene stratospheric wind patterns will be instrumental to further clarify dispersal patterns.

Conclusions

Given that Icelandic tephra layers provide critical age control for many locations in the northern North Atlantic and Europe, improving ages of and correlations between proximal and distal tephra deposits is vital. The ~ 12,000 cal a BP Vedde Ash has stood as an important age control point for the Late Glacial period by providing constraint for Greenland ice core records (Mortensen et al. 2005; Rasmussen et al. 2006), glacial geology and sea level curves (e.g., Norðdahl and Haflidason 1992; Rundgren et al. 1997; Farnsworth et al. 2022), paleoenvironmental records in Iceland, among other Northern Hemisphere localities (Björck et al. 1992; Rundgren 1995; Jennings et al. 2000; Geirsdóttir et al. 2022), the spatio-temporal evolution of abrupt North Atlantic climate change (Bakke et al. 2009; Lane et al. 2013), and regional paleoceanography and marine reservoir ages (e.g., Koç et al. 1993; Eiríksson et al. 2000, 2004; Xiao et al. 2017; Muschitiello et al. 2019). Building off Lane et al. (2012), the growing number of bimodal and silicic Katla tephra layers found during the Late Glacial to Early Holocene in Europe, and now locally in Iceland, increase temporal uncertainty when using the Vedde Ash without supporting age control. Detailed evaluations of prior Vedde Ash correlations are now required, especially if the records lack independent age control, which may result in revision of Late Glacial and Early Holocene paleoclimate events in the North Atlantic.

Supplementary Information The online version contains supplementary material available at https://doi.org/10.1007/s00445-023-01690-9.

Acknowledgements We kindly thank Þorsteinn Jónsson and Sveinbjörn Steinþórsson for lake coring assistance, Yarrow Axford for providing imagery of core 04-TORF-01, and Darrell Kaufman and Jordon Bright for performing ^{14}C analyses. We appreciate the constructive feedback from the editor (John Smellie), Alessio Di Roberto, Paul Zander, and one anonymous reviewer who contributed to improving the overall clarity of the manuscript.

Author contribution DJH, TT, ÁG, and GHM conceived the research; ÁG and GHM funded the research; ÁG, GHM, and CF acquired the lake sediment core; DJH and TT performed electron microprobe analyses; DJH performed age modeling and wrote the manuscript with contributions from all co-authors.

Funding This project has been supported by the Icelandic Center for Research (RANNÍS) through Grant-of-Excellences #022160002–04, #70272011–13, and #141573051–3 awarded to ÁG and GHM as well as through the University of Iceland Research Fund awarded to ÁG. DJH acknowledges support from RANNÍS Doctoral Student Grant #163431051 and NSF ARCSS #1836981, and CRF acknowledges support from the Doctoral Grant of the University of Iceland.

Declarations

Conflict of interest The authors declare no competing interests.

References

Alsos IG, Lammers Y, Kjellman SE, Merkel MKF, Bender EM, Rouillard A, Erlendsson E, Gudmundsdóttir ER, Benediktsson IÖ, Farnsworth WF, Brynjólfsson S, Gísladóttir G, Eddudóttir SD, Schomacker A (2021) Ancient sedimentary DNA shows rapid post-glacial colonisation of Iceland followed by relatively stable vegetation until the Norse settlement (Landnám) AD 870. Quat Sci Rev 259:106903. https://doi.org/10.1016/j.quascirev.2021.106903

Arnalds O (2004) Volcanic soils of Iceland. CATENA 56:3–20. https://doi.org/10.1016/j.catena.2003.10.002

Ascough PL, Cook GT, Hastie H, Dunbar E, Church MJ, Einarsson Á, McGovern TH, Dugmore AJ (2011) An Icelandic freshwater radiocarbon reservoir effect: implications for lacustrine ^{14}C chronologies. Holocene 21:1073–1080. https://doi.org/10.1177/0959683611400466

Axford Y, Miller GH, Geirsdóttir Á, Langdon PG (2007) Holocene temperature history of northern Iceland inferred from subfossil midges. Quat Sci Rev 26:3344–3358. https://doi.org/10.1016/j.quascirev.2007.09.003

Bakke J, Lie O, Heegaard E, Dokken T, Haug GH, Birks HH, Dulski P, Nilsen T (2009) Rapid oceanic and atmospheric changes during the Younger Dryas cold period. Nat Geosci 2:202–205. https://doi.org/10.1038/ngeo439

Birks HH, Gulliksen S, Haflidason H, Mangerud J, Possnert G (1996) New radiocarbon dates for the Vedde Ash and the Saksunarvatn Ash from western Norway. Quat Res 45:119–127. https://doi.org/10.1006/qres.1996.0014

Björck S, Ingólfsson Ó, Haflidason H, Hallsdóttir M, Andersen NH (1992) Lake Torfadalsvatn: a high resolution record of the North Atlantic ash zone I and the last glacial-interglacial environmental changes in Iceland. Boreas 21:15–22. https://doi.org/10.1111/j.1502-3885.1992.tb00009.x

Blaauw M, Christen JA (2011) Flexible paleoclimate age-depth models using an autoregressive gamma process. Bayesian Anal 6:457–474. https://doi.org/10.1214/11-BA618

Bond GC, Mandeville C, Hoffmann S (2001) Were rhyolitic glasses in the Vedde Ash and the North Atlantic's Ash Zone 1 produced by the same volcanic eruption? Quat Sci Rev 20:1189–1199. https://doi.org/10.1016/S0277-3791(00)00146-3

Boygle J (1999) Variability of tephra in lake and catchment sediments, Svínavatn. Iceland Glob Planet Change 21:129–149. https://doi.org/10.1016/S0921-8181(99)00011-9

Bronk Ramsey C (2009) Dealing with outliers and offsets in radiocarbon dating. Radiocarbon 51:1023–1045. https://doi.org/10.1017/S0033822200034093

Bronk Ramsey C (2023) OxCal v4.4, https://c14.arch.ox.ac.uk/oxcal/OxCal.html (last access: 9 March 2023).

Bronk Ramsey C, Albert PG, Blockley SPE, Hardiman M, Housley RA, Lane CS, Lee S, Matthews IP, Smith VC, Lowe JJ (2015) Improved age estimates for key Late Quaternary European tephra horizons in the RESET lattice. Quat Sci Rev 118:18–32. https://doi.org/10.1016/j.quascirev.2014.11.007

Carey RJ, Houghton BF, Thordarson T (2010) Tephra dispersal and eruption dynamics of we and dry phases of the 1875 eruption of Askja Volcano. Iceland Bull Volcanol 72:259–278. https://doi.org/10.1007/s00445-009-0317-3

Cook E, Abbott PM, Pearce NJG, Mojtabavi S, Svensson A, Bourne AJ, Rasmussen SO, Seierstad IK, Vinther BM, Harrison J, Street E, Steffensen JP, Wilhelms F, Davies SM (2022) Volcanism and the Greenland ice cores: a new tephrochronological framework for the last glacial-interglacial transition (LGIT) based on cryptotephra deposits in three ice cores. Quat Sci Rev 292:107595. https://doi.org/10.1016/j.quascirev.2022.107596

Davies SM, Turney CS, Lowe JJ (2001) Identification and significance of a visible, basalt-rich Vedde Ash layer in a Late-glacial sequence on the Isle of Syke, Inner Hebrides. Scotland J Quat Sci 16:99–104. https://doi.org/10.1002/jqs.611

Dugmore AJ, Cook GT, Shore JS, Newton AJ, Edwards KJ, Larsen G (1995) Radiocarbon dating tephra layers from Britain and Iceland. Radiocarbon 37:379–388. https://doi.org/10.1017/S0033822200003085X

Eiríksson J, Knudsen KL, Haflidason H, Henriksen P (2000) Late-glacial and Holocene palaeoceanography of the North Icelandic shelf. J Quat Sci 15:23–42. https://doi.org/10.1002/(SICI)1099-1417(200001)15:1%3c23::AID-JQS476%3e3.0.CO;2-8

Eiríksson J, Larsen G, Knudsen KL, Heinemeier J, Símonarson LA (2004) Marine reservoir age variability and water mass distribution in the Iceland Sea. Quat Sci Rev 23:2247–2268. https://doi.org/10.1016/j.quascirev.2004.08.002

Farnsworth WR, Ingólfsson Ó, Mannerfelt ES, Kalliokoski MH, Guðmundsdóttir ER, Retelle M, Allaart L, Brynjólfsson S, Furze MF, Hancock HJ, Kjær KH, Pienkowski AJ, Schomacker A (2022) Vedde Ash constrains Younger Dryas glacier re-advance and rapid glacio-isostatic rebound on Svalbard. Quat Sci Adv 5:100041. https://doi.org/10.1016/j.qsa.2021.10004

Florian CR (2016) Multi-proxy reconstructions of Holocene environmental change and catchment biogeochemistry using algal pigments and stable isotopes preserved in lake sediment from Baffin Island and Iceland. PhD thesis, University of Colorado Boulder and University of Iceland.

Flóvenz ÓG, Sæmundsson K (1993) Heat flow and geothermal processes in Iceland. Tectonophysics 225:123–138. https://doi.org/10.1016/0040-1951(93)90253-G

Geirsdóttir Á, Hardardóttir J, Sveinbjornsdóttir ÁE (2000) Glacial extent and catastrophic meltwater events during the deglaciation of Southern Iceland. Quat Sci Rev 19:1749–1761. https://doi.org/10.1016/S0277-3791(00)00092-5

Geirsdóttir Á, Miller GH, Thordarson T, Ólafsdóttir KB (2009) A 2000 year record of climate variations reconstructed from Haukadalsvatn, West Iceland. J Paleolimnol 41:95–115. https://doi.org/10.1007/s10933-008-9253-z

Geirsdóttir Á, Harning DJ, Miller GH, Andrews JT, Zhong Y, Caseldine C (2020) Holocene history of landscape instability in Iceland: can we deconvolve the impacts of climate, volcanism and human activity? Quat Sci Rev 249:106633. https://doi.org/10.1016/j.quascirev.2020.106633

Geirsdóttir Á, Miller GH, Harning DJ, Hannesdóttir H, Thordarson T, Jónsdóttir I (2022) Recurrent outburst floods and explosive volcanism during the Younger Dryas-Early Holocene deglaciation in south Iceland: evidence from a lacustrine record. J Quat Res 37:1006–1023. https://doi.org/10.1002/jqs.3344

Gudmundsdóttir ER, Eiríksson J, Larsen G (2011) Identification and definition of primary and reworked tephra in Late Glacial and Holocene marine shelf sediments off North Iceland. J Quat Sci 26:589–602. https://doi.org/10.1002/jqs.1474

Gudmundsdóttir ER, Larsen G, Eiríksson J (2012) Tephra stratigraphy on the North Icelandic shelf: extending tephrochronology into marine sediments off North Iceland. Boreas 41:719–734. https://doi.org/10.1111/j.1502-3885.2012.00258.x

Haflidason H, Regnéll C, Pyne-O'Donnell S, Svendsen JI (2018) Extending the known distribution of the Vedde Ash into Siberia: occurrence in lake sediments from the Timan Ridge and the Ural Mountains, northern Russia. Boreas 48:444–451. https://doi.org/10.1111/bor.12354

Harning DJ, Geirsdóttir Á, Miller GH, Zalzal K (2016) Early Holocene deglaciation of Drangajökull, Vestfirðir. Iceland Quat Sci Rev 153:192–198. https://doi.org/10.1016/j.quascirev.2016.09.030

Harning DJ, Thordarson T, Geirsdóttir Á, Zalzal K, Miller GH (2018) Provenance, stratigraphy and chronology of Holocene tephra from Vestfirðir. Iceland Quat Geochron 46:59–76. https://doi.org/10.1016/j.quageo.2018.03.007

Harning DJ, Thordarson T, Geirsdóttir Á, Ólafsdóttir S, Miller GH (2019) Marker tephra in Haukadalsvatn lake sediment: a key to the Holocene tephra stratigraphy of Northwest Iceland. Quat Sci Rev 219:154–170. https://doi.org/10.1016/j.quascirev.2019.07.019

Jennings A, Syvitski J, Gerson L, Grönvold K, Geirsdóttir Á, Hardardóttir J, Andrews J, Hagen S (2000) Chronology and paleoenvironments during the late Weichselian deglaciation of the southwest Iceland shelf. Boreas 29:167–183. https://doi.org/10.1111/j.1502-3885.2000.tb00976.x

Jennings AE, Thordarson T, Zalzal K, Stoner J, Hayward C, Geirsdóttir Á, Miller GH (2014) Holocene tephra from Iceland and Alaska in SE Greenland Shelf Sediments. In: Austin, W.E.N., Abbott, P.M., Davies, S.M., Pearce, N.J.G., and Wastegård, S. (eds) *Marine Tephrochronology*. Geological Society, London, Specical Publications, 398. https://doi.org/10.1144/SP398.6

Jones G, Lane CS, Brauer A, Davies SM, De Bruijn R, Engels S, Haliuc A, Hoek WZ, Merkt J, Sachse D, Turner F, Wagner-Cremer F (2018) The Lateglacial to early Holocene tephrochronological record from Lake Hämelsee, Germany: a key site within the European tephra framework. Boreas 47:28–40. https://doi.org/10.1111/bor.12250

Koç N, Jansen E, Haflidason H (1993) Paleoceanographic reconstructions of surface ocean conditions in the Greenland, Iceland and Norwegian Seas through the last 14 ka based on diatoms. Quat Sci Rev 12:115–140. https://doi.org/10.1016/0277-3791(93)90012-B

Koren JH, Svendsen JI, Mangerud J, Furnes H (2008) The Dimna Ash – a 12.8 ^{14}C ka-old volcanic ash in Western Norway. Quat Sci Rev 27:85–94. https://doi.org/10.1016/j.quascirev.2007.04.021

Kristjánsdóttir GB, Stoner JS, Jennings AE, Andrews JT, Grönvold K (2007) Geochemistry of Holocene cryptotephras from the North Iceland Shelf (MD99-2269): intercalibration with radiocarbon and palaeomagnetic chronostratigraphies. Holocene 17:155–176. https://doi.org/10.1177/0959683607075829

Lacasse C (2001) Influence of climate variability on the atmospheric transport of Icelandic tephra in the subpolar North Atlantic. Glob Planet Change 29:31–55. https://doi.org/10.1016/S0921-8181(01)00099-6

Lacasse C, Sigurdsson H, Johannesson H, Paterne M, Carey S (1995) Source of ash-zone-1 in the North-Atlantic. Bull Volcanol 57:18–32. https://doi.org/10.1007/BF00298704

Lacasse C, Werner R, Paterne M, Sigurdson H, Carey S, Pinte G (1998) Long-range transport of Icelandic tephra to the Irminger Basin,

Site 919. In: Saunders, A.D., Larsen, H.C., Wise Jr., S.W. (Eds.), Proceedings of the Ocean Drilling Program. Scientific Results, 152, 51–65. https://doi.org/10.2973/odp.proc.sr.152.205.1998

Lane CS, Andric M, Cullen VL, Blockley SPE (2011) The occurrence of distal Icelandic and Italian tephra in the Lateglacial of Lake Bled. Slovenia Quat Sci Rev 30:1013–1018. https://doi.org/10.1016/j.quascirev.2011.02.014

Lane CS, Blockley SPE, Mangerud J, Smith VC, Lohne ØS, Tomlinson EL, Matthews IP, Lotter AF (2012) Was the 12.1 ka Icelandic Vedde Ash one of a kind? Quat Sci Rev 33:87–99. https://doi.org/10.1016/j.quascirev.2011.11.011

Lane CS, Brauer A, Blockley SPE, Dulski P (2013) Volcanic ash reveals time-transgressive abrupt climate change during the Younger Dryas. Geology 41:1251–1254. https://doi.org/10.1130/G34867.1

Larsen DJ, Miller GH, Geirsdóttir Á, Ólafsdóttir S (2012) Non-linear Holocene climate evolution in the North Atlantic: a high-resolution, multi-proxy record of glacier activity and environmental change from Hvítárvatn, central Iceland. Quat Sci Rev 39:14–25. https://doi.org/10.1016/j.quascirev.2012.02.006

Leahy K (1997) Discrimination of reworked pyroclastics from primary tephra-fall tuffs: a case study using kimberlites of Fort a la Corne, Saskatchewan. Canada Bull Volcanol 59:65–71. https://doi.org/10.1007/s004450050175

Lowe DJ (2011) Tephrochronology and its application: A review. Quat Geochron 6:107–153. https://doi.org/10.1016/j.quageo.2010.08.003

MacLeod A, Matthews IP, Lowe JJ, Palmer AP, Albert PG (2015) A second isochron for the Younger Dryas period in northern Europe: the Abernethy Tephra. Quat Geochron 28:1–11. https://doi.org/10.1016/j.quageo.2015.03.010

Matthews IP, Birks HH, Bourne AJ, Brooks SJ, Lowe JJ, Macleod A, Pyne-O'Donnell SDF (2011) New age estimates and climatostratigraphic correlations for the Borrobol and Penifiler Tephras: evidence from Abernethy Forest. Scotland J Quat Sci 26:247–252. https://doi.org/10.1002/jqs.1498

Mangerud J, Andersen ST, Berglund BE, Donner JJ (1974) Quaternary stratigraphy of Norden, a proposal for terminology and classification. Boreas 3:109–128. https://doi.org/10.1111/j.1502-3885.1974.tb00669.x

Mangerud J, Lie SE, Furnes H, Kristiansen IL, Lømo L (1984) A Younger Dryas Ash bed in Western Norway, and its possible correlations with tephra in cores from the Norwegian Sea and the North Atlantic. Quat Res 21:85–104. https://doi.org/10.1016/0033-5894(84)90092-9

Mortensen AK, Bigler M, Grönvold K, Steffensen JP, Johnsen SJ (2005) Volcanic ash layers from the Last Glacial Termination in the NGRIP ice core. J Quat Sci 20:209–219. https://doi.org/10.1002/jqs.908

Muschitiello F, D'Andrea WJ, Schmittner A, Heaton TJ, Balascio NL, deRoberts N, Caffee M, Woodruff TE, Welten KC, Skinner LC, Simon MH, Dokken TM (2019) Deep-water circulation changes lead North Atlantic climate during deglaciation. Nat Comm 10:1–10. https://doi.org/10.1038/s41467-019-09237-3

Norðdahl H, Haflidason H (1992) The Skógar Tephra, a Younger Dryas marker in North Iceland. Boreas 21:23–41. https://doi.org/10.1111/j.1502-3885.1992.tb00010.x

Óladóttir BA, Sigmarsson O, Larsen G, Devidal J-L (2011) Provenance of basaltic tephra from Vatnajökull subglacial volcanoes, Iceland, as determined by major- and trace-element analyses. Holocene 21:1037–1048. https://doi.org/10.1177/0959683611400456

Óladóttir BA, Thordarson T, Geirsdóttir Á, Jóhannsdóttir GE, Mangerud J (2020) The Saksunarvatn Ash and the G10ka series tephra. Review and current state of knowledge. Quat Geochron 56:101041. https://doi.org/10.1016/j.quageo.2019.101041

Patton H, Hubbard A, Bradwell T, Schomacker A (2017) The configuration, sensitivity and rapid retreat of the Late Weichselian Icelandic ice sheet. Earth-Sci Rev 166:223–245. https://doi.org/10.1016/j.earscirev.2017.02.001

Pilcher J, Bradley RS, Francus P, Anderson L (2005) A Holocene tephra record from the Lofoten Islands, Arctic Norway. Boreas 34:136–156. https://doi.org/10.1111/j.1502-3885.2005.tb01011.x

R Core Team (2021) R: A language and environment for statistical computing. Vienna, Austria: R Foundation for Statistical Computing, https://www.R-project.org/.

Rasmussen SO, Andersen KK, Svensson AM, Steffensen JP, Vinther BM, Clausen HB, Siggaard-Andersen M-L, Johnsen SJ, Larsen LB, Dahl-Jensen D, Bigler M, Röthlisberger R, Fischer H, Goto-Azuma K, Hansson ME, Ruth U (2006) A new Greenland ice core chronology for the last glacial termination. J Geophys Res 111:1–16. https://doi.org/10.1029/2005JD006079

Reimer PJ, Austin WEN, Bard E, Bayliss A, Blackwell PG, Bronk Ramsey C, Butzin M, Cheng H, Edwards RL, Friedrich M, Grootes PM, Guilderson TP, Hajdas I, Heaton TJ, Hogg AG, Hughen KA, Kromer B, Manning SW, Muscheler R, Palmer JG, Pearson C, van der Plicht J, Reimer RW, Richards DA, Scott EM, Southon JR, Turney CSM, Wacker L, Adolphi F, Büntgen U, Capano M, Fahri SM, Fogtmann-Schulz A, Friedrich R, Köhler P, Kudsk S, Miyake F, Olsen J, Reinig F, Sakamoto M, Sookdeo A, Talamo S (2020) The IntCal20 northern hemisphere radiocarbon age calibration curve (0–55 cal kBP). Radiocarbon 62:725–757. https://doi.org/10.1017/RDC/2020.41

Rundgren M (1995) Biostratigraphic evidence of the Allerød-Younger Dryas-Preboreal Oscillation in Northern Iceland. Quat Res 44:405–416. https://doi.org/10.1006/qres.1995.1085

Rundgren M, Ingólfsson Ó, Björck S, Jiang H, Haflidason H (1997) Dynamic sea-level change during the last deglaciation of northern Iceland. Boreas 26:201–215. https://doi.org/10.1111/j.1502-3885.1997.tb00852.x

Shane PAR, Sikes EL, Guilderson TP (2006) Tephra beds in deep-sea cores off northern New Zealand: implications for the history of Taupo volcanic zone, Mayor Island and White Island volcanoes. J Volcanol Geotherm Res 154:276–290. https://doi.org/10.1016/j.jvolgeores.2006.03.021

Sharma K, Self S, Blake S, Thordarson T, Larsen G (2008) The AD 1362 Öræfujökull eruption, S.E. Iceland: Physical volcanology and volatile release. J Volcanol Geotherm Res 178:719–739. https://doi.org/10.1016/j.jvolgeores.2008.08.003

Stuiver M, Polach HA (1977) Discussion reporting of ^{14}C data. Radiocarbon 19:35–363. https://doi.org/10.1017/S0033822200003672

Thorarinsson S (1950) The eruption of Mt. Hekla 1947–1948. Bulletin Volcanologique 10:157–168. https://doi.org/10.1007/BF02596085

Thornalley DJR, McCave IN, Elderfield H (2011) Tephra in deglacial ocean sediments south of Iceland: stratigraphy, geochemistry and oceanic reservoir ages. J Quat Sci 26:190–198. https://doi.org/10.1002/jqs.1442

Tomlinson EL, Thordarson T, Lane CS, Smith VC, Manning CJ, Müller W, Menzies MA (2012) Petrogenesis of the Sólheimar ignimbrite (Katla, Iceland): implications for tephrostratigraphy. Geochim Cosmochim Acta 86:318–337. https://doi.org/10.1016/j.gca.2012.03.012

Voelker AHL, Haflidason H (2015) Refining the Icelandic tephrachronology of the last glacial period – the deep-sea core PS2644 record from the southern Greenland Sea. Glob Planet Change 131:35–62. https://doi.org/10.1016/j.gloplacha.2015.05.001

Wastegård S (2002) Early to middle Holocene silicic tephra horizons from the Katla volcanic system, Iceland: new results from the Faroe Islands. J Quat Sci 17:723–730. https://doi.org/10.1002/jqs.724

Wastegård S, Björck S, Possnert G, Wohlfarth B (1998) Evidence of the occurrence of Vedde Ash in Sweden: radiocarbon age estimates. J Quat Sci 13:271–274. https://doi.org/10.1002/(SICI)1099-1417(199805/06)13:3%3c271::AID-JQS372%3e3.0.CO;2-4

Wilcox RE, Naeser CW (1992) The Pearlette family ash beds in the Great Plains: finding their identities and their roots in the Yellowstone country. Quat Int 13–14:9–13

Xiao X, Zhao M, Knudsen KL, Longbin S, Eiríksson J, Gudmundsdóttir E, Jiang H, Guo Z (2017) Deglacial and Holocene sea-ice variability north of Iceland and response to ocean circulation changes. Earth Planet Sci Lett 472:14–24. https://doi.org/10.1016/j.epsl.2017.05.006